

SUPPLEMENTAL MATERIAL

Supplemental Methods:

Differential Scanning Calorimetry (DSC) Lipid films were made by dissolving appropriate amounts of lipids in chloroform/methanol (2/1), followed by evaporation of the solvent under nitrogen to deposit the lipid film on the wall of a test-tube. Dried lipid films were hydrated in KHE buffer, and suspended by vigorous vortexing for a few minutes below 50°C to facilitate hydration of the sample. DSC measurements were carried in a NanoII differential scanning calorimeter (Calorimetry Sciences Corporation, Lindon, UT). The scan rate was 1 deg.C/min-1 with a delay of 5 min between sequential scans in a series to allow for thermal equilibration. DSC curves were analyzed by the fitting program DA-2 provided by Microcal Inc. (Northampton, MA). Liposome concentration was 1 mM, and cell volume was 340 μ l.

Assays with Giant Unilamellar Vesicles (GUV)- GUVs were prepared by electroformation. A PRETGUV 4 Chamber supplied by Industrias Técnicas ITC (Bilbao, Spain) was used for vesicle preparation. Stock solutions of lipids (0.2 mg/ml total lipid, 0.2 mol% DiI) were prepared in a chloroform:methanol (9:1, v/v) solution. Three microlitres of the appropriate lipid stocks were added on the surface of Pt electrodes and solvent traces were removed by evacuating the chamber under high vacuum for 2 h. The Pt electrodes were covered with 400 μ l of 10 mM HEPES, pH 7.4. The Pt wires were connected to an electric wave generator (TG330 function generator, Thurlby Thandar Instruments, Huntington, UK) under AC field conditions (10 Hz, 1 V) for 2 h at 60 °C. For GUV observation at room temperature, a chamber supplied by L.A. Bagatolli (Odense, Denmark) was used allowing direct GUV visualization under the microscope. After GUV formation, the chambers were located in an inverted confocal fluorescence microscope (Nikon D-ECLIPSE C1, Nikon Inc., Melville, NY). Excitation wavelength was 561 nm for DiI. The images were collected using a band-pass filter of 593 ± 20 nm. Image treatment and quantification was performed using EZ-C1 3.20 software.

Dynamic light scattering (DLS) measurements-Vesicle size was determined by DLS at a fixed angle of 90° and 37°C, using a Protein Solutions DynaPro instrument equipped with a temperature-controlled microchamber and a 64-channel correlator capable of estimating particle sizes in the range from 5 nm to 5000 nm. LUV (50 μ M) were incubated with or without proteins in KHE buffer for 10 min at 37°C under constant stirring using an Eppendorf thermomixer ($V_{\text{final}}=70$ μ l), followed by DLS analysis. Each measurement was done as an average of 20 data points, and took approximately between 15-20 min. Data were analyzed by the cumulant method using the software provided by the instrument.

Supplemental Figures

SUPPLEMENTAL FIGURE 1. Dose-dependence effects of CL on liposome permeabilization induced by different agents. Liposomes loaded with ANTS/DPX containing increasing amounts of CL were treated with indicated proteins/peptides, and final extents of vesicular contents release were determined when the fluorescence signal reached a plateau. BAK Δ C, tBID, tetanolysin, and melittin concentrations were 200 nM, 100 nM, 10nM, and 1000 nM, respectively. Starting lipid compositions were 55PC/35PE/10PI except for tetanolysin (50PC/50CHOL). In all cases, PC was substituted for increasing amounts of CL. Data represent mean values and S.E of 2-5 independent experiments.

SUPPLEMENTAL FIGURE 2. Specificity of CL's effect on the lipid-interacting properties of BAK Δ C. A, Plot of immunoblot response of BAK Δ C quantified by densitometry versus protein concentration. Dashed line represents least-squares linear fit to the experimental data ($R^2=0.94$). B, Quantitation of BAK Δ C binding to liposomes under different conditions assessed by densitometric analysis of immunoblot. Total BAK Δ C concentrations used in liposome-binding studies were within the linear range shown in Panel A (typically, 15-30 ng). Data correspond to mean values and S.E obtained from 2-4 independent measurements. C,

Quantitation of BAK Δ C oligomerization under different conditions determined by Superdex 200 gel-filtration chromatography and immunoblotting as shown in Figure 2C. Data correspond to mean values and S.E for 2-4 independent experiments.

SUPPLEMENTAL FIGURE 3. Representative cryo-EM images of selected samples prepared as described in Figure 8 Panels Ai-Ci.

SUPPLEMENTAL FIGURE 4. Effect of incorporating LPC/DAG on different properties of CL-enriched MOM-like LUV. A, Effect of LPC and DAG on tetanolysin-mediated liposome permeabilization. ANTS/DPX containing LUV were prepared composed of 50PC/50CHOL (30CL Lipos.), 40PC/50CHOL/10LPC (+10%LPC), or 40PC/50CHOL/10DAG (+10%DAG), followed by addition of indicated amounts of tetanolysin. B, LPC and DAG do not change lateral distribution of lipids in CL-enriched LUV, as assessed by DSC. As a positive control, substituting mirystoylCL for heart CL led to segregation of lipids into distinct domains. C, Effect of LPC and DAG on lateral lipid distribution and global liposome morphology, as assessed by confocal microscopy analysis of GUV containing DiI. GUV were composed of 25PC/35PE/30CL/10PI (Control) 25PC/25PE/30CL/10PI/10LPC (+10LPC), or 25PC/25PE/30CL/10PI/10DAG (+10DAG). White bars correspond to 5 μ m.

Supplemental Table I. EC₅₀ (nM) values for tBID activation of BAK Δ C-triggered vesicular ANTS/DPX release

<i>Protein</i>	<i>BAKΔC+tBID</i>	<i>BAKΔC+tBID</i>	<i>BAKΔC+tBIDmt</i>	<i>BAKΔCmt+tBID</i>
EC ₅₀	872.5 \pm 48.1	68.3 \pm 9.1	784.7 \pm 33.5	1271.3 \pm 32.3

Mean EC₅₀ values were inferred by fitting experimental data shown in Fig. 1 C with a sigmoidal dose-response nonlinear regression model. Errors are given to indicate the quality of the fits. tBIDmt=tBID(93-96)A; BAK Δ Cmt=BAK Δ CG126S.

Supplemental Table II. EC₅₀ (pmol) values obtained for BAK Δ C:lipid binding determined from dot blot lipid overlay studies

<i>Lipid</i>	<i>CL</i>	<i>PG</i>	<i>PI</i>	<i>PC</i>
EC ₅₀ (pmol)	411.3 \pm 51.2	1932.6 \pm 87.0	4874.2 \pm 123.1	>10.000

EC₅₀ values were inferred by fitting experimental data shown in Fig. 3 C with a sigmoidal dose-response nonlinear regression model. Errors are given to indicate the quality of the fits.

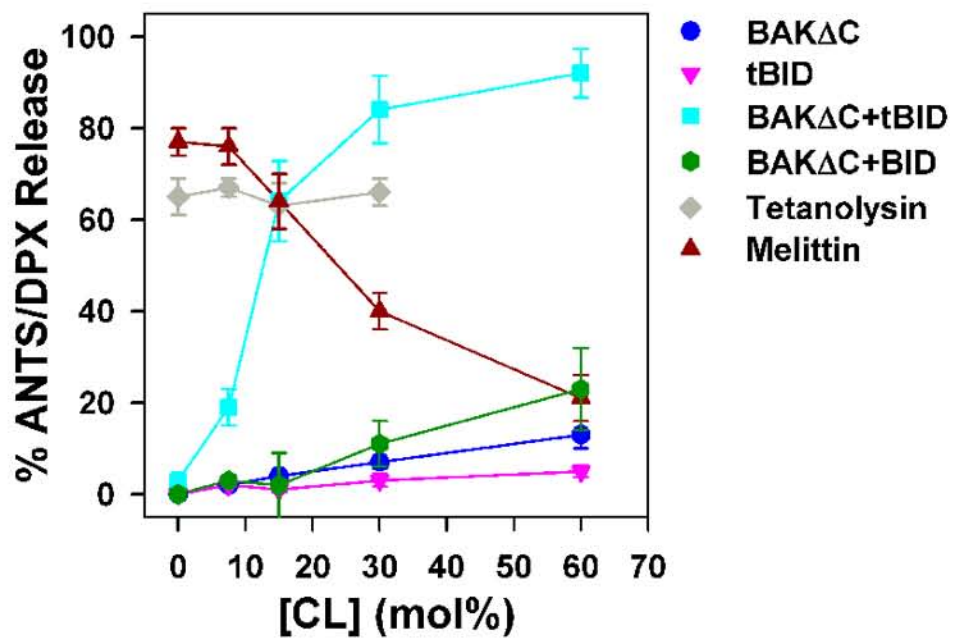
Supplemental Table III. Dissociation Constants and Thermodynamic parameters determined by ITC for 29mer BID BH3 peptide binding to BCL-XL Δ C at 303K

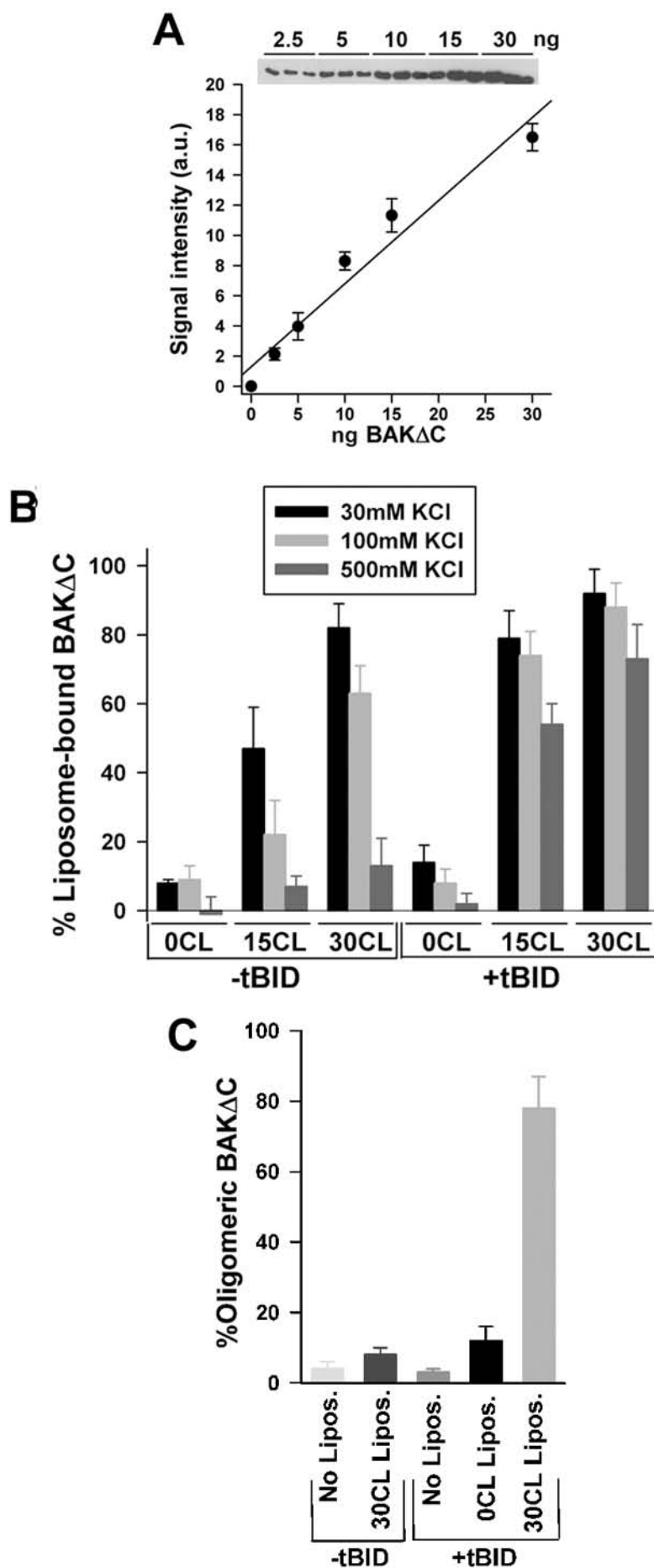
<i>Receptor</i>	<i>K_d</i> (nM)	<i>ΔG</i> (Kcal/mol)	<i>ΔH</i> (Kcal/mol)	<i>TΔS</i> (Kcal/mol)	<i>n</i>
BCL-XL Δ C	44.3 \pm 1.6	-10.11	-12.31 \pm 0.4	-4.82	0.99 \pm 0.3

Supplemental Table IV: Effect of different lipids on various liposome properties

<i>Composition^a</i>	<i>PC/PE/PI/CL</i>	<i>PC/PE/PI/mCL</i>	<i>PC/PE/PI/CL/LPC</i>	<i>PC/PE/PI/CL/DAG</i>
T($^{\circ}$ C) ^b	Not detected	38.3	Not detected	Not detected
Size ^c	147.2 \pm 24.3	143.6 \pm 32.2	138.6 \pm 28.1	161.5 \pm 41.1

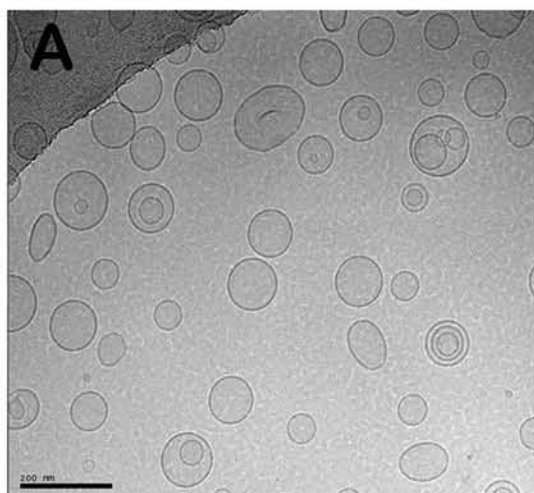
^aLipid compositions were as follows (mol percent), PC/PE/PI/CL= 25PC/35PE/10PI/30CL; PC/PE/PI/mCL= 25PC/35PE/10PI/30MirCL; PC/PE/PI/CL/LPC= 20PC/30PE/10PI/30CL/10LPC; PC/PE/PI/CL/DAG= 20PC/30PE/10PI/30CL/10DAG; ^bTransition temperatures of multilamellar vesicles of indicated lipid composition as determined by DSC. ^cSize distribution of LUV of indicated lipid composition determined by QELS.



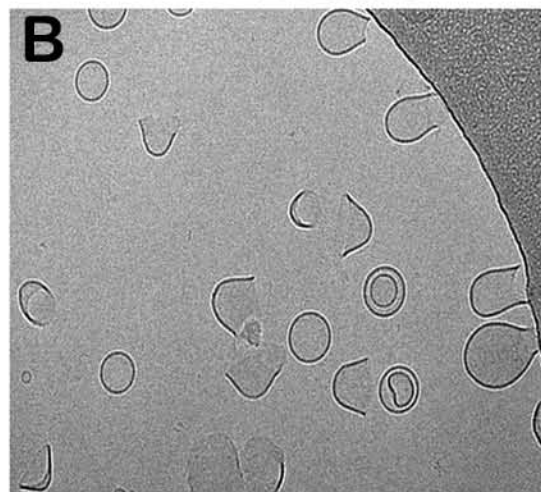


Supplemental Figure 2

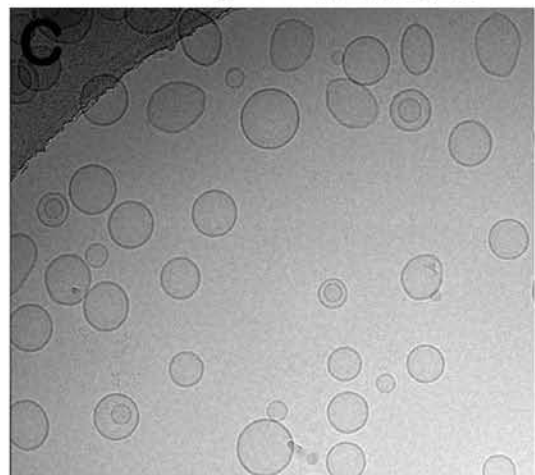
30CL Lipos.



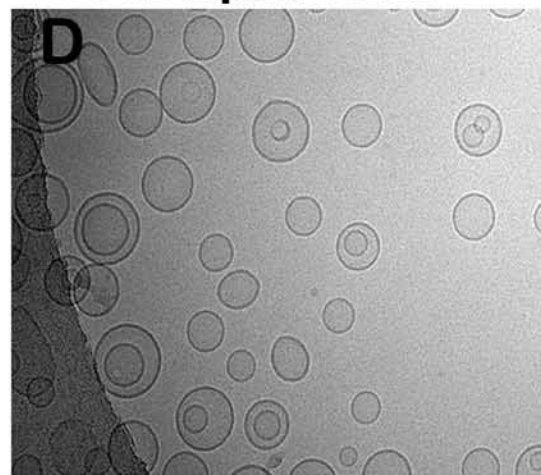
30CL Lipos.+BAK Δ C+tBID



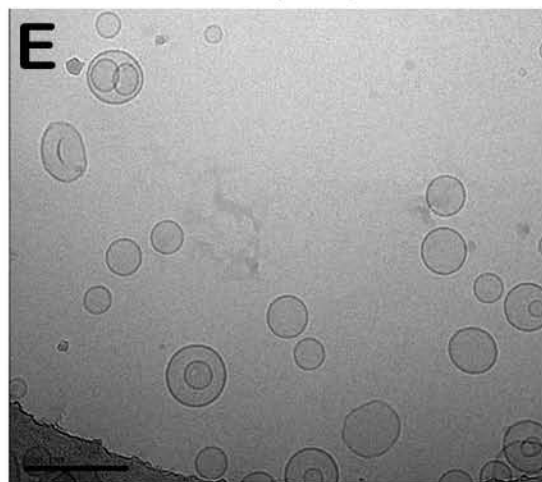
30CL Lipos.+BAK Δ C



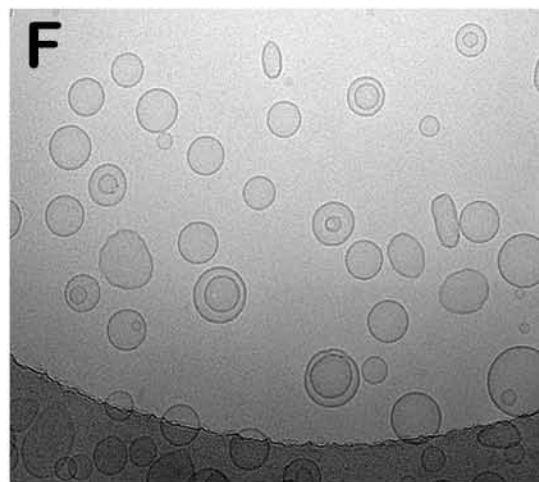
30CL Lipos.+tBID

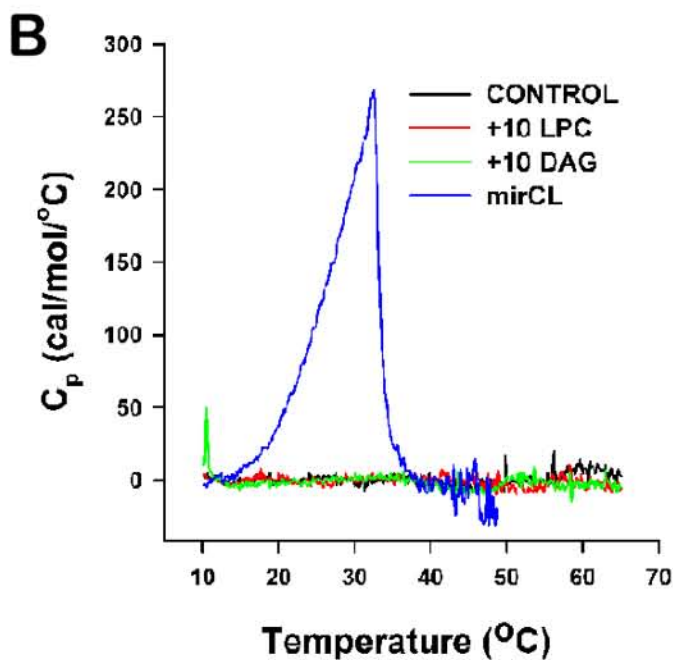
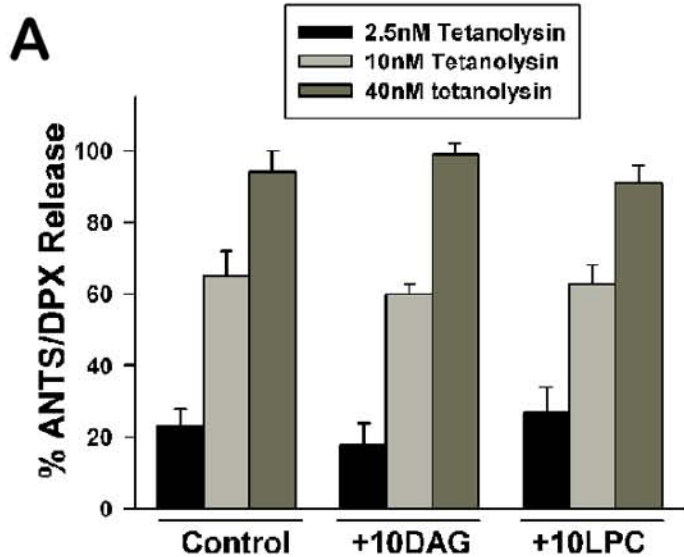


0CL Lipos,



0CL Lipos,+BAK Δ C+tBID





C

30CL Lipos.

+10DAG

+10LPC

